JOURNAL OF MATERIALS SCIENCE **36** (2001) 5649–5657

The structural transitions during leaching of Ni_2Al_3 phase in a Raney Ni-Al alloy

RONG WANG, ZHILONG LU, TSUN KO
Department of Materials Physics, University of Science and Technology Beijing, Beijing 100083, People's Republic of China; Laboratory of Atomic Imaging of Solids, Institute of Metal Research, Chinese Academy of Sciences, Shenyang 110015, People's Republic of China

The microstructure transitions during leaching of a rapidly solidified Ni-Al alloy have been investigated by means of X-ray diffraction, transmission electron microscopic (TEM) and high resolution electron microscopic (HREM) techniques. Ni_2Al_3 was the main phase in the starting Ni-Al alloy. The microstructure of the Raney nickel catalyst consists of nano-scale nickel crystallites, residue of source phases surrounded by nano-scale boundary regions. The transformation during leaching of Ni_2Al_3 phase was an advancing interface type process. Clusters of AuCu-structure type face-centrered tetragonal Ni_3Al_2 as an intermediate phase seems to appear in the reaction front. Based on an analysis of the atomic configurations of phases Ni_2Al_3, Ni_3Al_2 and nickel, a reasonable explanation for the transition mechanism during leaching of Ni_2Al_3 phase and the arc characteristic of diffraction spots was proposed. The nickel crystallites generated during leaching obey an orientation relationship with the source Ni_2Al_3 phase, which is consistent with the Delannay's orientation relationship proposed for nickel and NiAl phases. The nano-scale structural characteristic of the Raney nickel catalyst, especially its porous structure at the boundary regions, provides an excellent hydrogenation catalytic activity and selectivity of the catalyst.

1. Introduction

Since the first discovery of the Raney nickel catalyst about 70 years ago, understanding of the structural changes which take place in the Raney source phases during leaching has been accumulated greatly. Raney nickel catalyst is obtained by leaching aluminium (silicon) out of a Ni-Al (Ni-Si) alloy with an alkali solution and both $NiAl_3$ and Ni_2Al_3 are the important source phases existing in the Ni-Al alloy for producing the catalyst. It was thought in the early works [1, 2] that the original lattice of Ni_2Al_3 was kept up during leaching. A large number of the vacancies produced in the process made the structure of the catalyst, in which nickel atoms stayed still its own original lattice sides, more porous. Consequently the catalyst used to be called "the skeleton nickel catalyst". Before long, a common understanding [3] was accepted on the basis of the studies of X-ray and electron diffraction that the nickel atoms in the original source phases were rearranged into the lattice of nickel phase after the leaching treatment. The grain size of the nickel phase was determined by X-ray diffraction to be nano-scale [3]. Freel *et al*. [4] proposed an "advancing interface" type process for the removal of aluminium from both $NiAl_3$ and Ni_2Al_3 source phases, i.e. the removal of aluminium was not a progressive process over the whole particles. There was a sharp concentration gradient of aluminium to be detected by electron probe microanalysis between an unattacked area in the alloy and the adjoining activated area, the area rich in voids in front of the reaction [4]. Bakker *et al*. [5] suggested as well that the leaching sequence of Ni_2Al_3 be not one of dissolution and precipitation but a preferential dissolution followed by reconstruction.

Concerning whether the removal of aluminium advanced via intermediate compounds, there are quite different opinions. The view that none of intermediate compounds be formed during leaching of the equilibrium intermetallics Ni_2Al_3 was held by some researchers [4–7]. The nickel crystallites newly generated were considered coexisting with the source phase Ni_2Al_3 in the microstructure under the condition of incomplete leaching [5]. Hamer-Thibault *et al*. [7] investigated the microstructures of the leaching products from a rapidly solidified Ni-Al alloy. By means of TEM and HREM techniques, they showed that, corresponding to two main regions of the precursor microstructure, Ni_2Al_3 and NiAl, nickel crystallites were obtained separately according to respective orientation relationship between nickel and the precursor phase. Thus the idea of existence of the intermediate phase NiAl at the reaction front from Ni_2Al_3 source phase to nickel product seemed to be abandoned. The areas leached proved to possess a sponge-like formation, in which embedded the newly generated nickel crystallites.

Delannay [8] gave an opposite opinion about the phase transformation process during leaching of Ni_2Al_3

phase. A layer of NiAl was reported to be detected at the interfacial area between Ni_2Al_3 and nickel and the formation of NiAl was thought to prevent further leaching of this type of alloy. And, from this, the reason was given why the aluminium concentration in a fully leached Raney nickel alloy exceeded the solubility limit. Additionally, another intermediate phase Ni_3Al was proposed by the author to be present as well in the process. However, none of definite experimental evidences was provided to support the proposition about existence of Ni_3Al. An orientation relationship between nickel crystallites and the NiAl crystal was proposed [8, 9] as two of the three equivalent {1 0 0} planes of nickel parallel to two of the six {0 1 1} planes of NiAl whereas the third is parallel to a (1 0 0) plane of NiAl. It is just the same as the Bain relationship between face centered cubic and body centered cubic structures and involves the smallest strain in a transformation sequence. No suggestion has been made for any long distant movement of atoms in the transition mechanism from the intermediate NiAl compound to the product nickel crystallite during leaching [9]. It should be noted that Ni_2Al_3 is a vacancy-ordered phase based on the structure of NiAl. And as realized already by the author [8], all of the reflections of NiAl are superimposed on reflections of Ni_2Al_3. Thus, it is impossible to identify the phase detected to be NiAl and not Ni_2Al_3 phase unambiguously just from an individual electron diffraction pattern.

The point of view of existence of intermediate phases during a leaching sequence was also held by Gros *et al*. [9, 10]. In their proposition, the ordered hexagonal structure of Ni_2Al_3 was destroyed at the beginning of leaching, a disordered cubic-NiAl structure, or Ni_2Al, formed next and finally nickel crystallites. Different authors had reported that Ni_2Al phase had a body-centered tetragonal Ni_3Al_2 structure [11, 12], the content of nickel was 60–66.6 at.%. However, the electron diffraction pattern, which Gros *et al*. had presented [9, 10], looks like a composite of two oriented domains of the Ni_2Al_3 phase. Ivanov *et al*. [13, 14] discovered that a mixture of cubic nickel and CsCl-type structure was identified by X-ray diffraction in a Raney Ni catalyst obtained by leaching of a mechanically alloyed material containing 35 at.% Ni and 65 at.% Al. The starting alloy was reported to have a CsCl-type NiAl structure.

In the present work, an investigation has been carried out to discover the transformation sequence during leaching of a rapidly solidified Ni-Al alloy by means of X-ray diffraction, transmission electron microscopic (TEM) and high resolution electron microscopic (HREM) techniques. A deeper insight on the transformation sequence and the crystallography during leaching of $NiAl_3$ phase in a commercial Raney alloy has been reported elsewhere [15]. This paper deals with the microstructure changes during aluminium leaching of Ni_2Al_3 source phase.

2. Experiments

A rapidly solidified Ni-Al alloy was prepared by melt-spinning, its composition shown in Table I. Pieces of the ribbon were ground into a powder as fine as possible and treated at 30°, 50°, 70° and 90°C for 0.5, 1.5 and 2.5 hours in a 20% sodium hydroxide solution. The powder after leaching was washed with de-ionized water and ethanol in turn and stored in ethanol to prevent oxidation.

TABLE I The composition of the rapidly solidified Raney Ni-Al alloy (wt%)

Ni	Al	Fe	Mg	Ca	P
48.27	47.64	0.80	0.01	0.030	3.25

The powders before and after leaching were identified by X-ray diffraction with Cu Kα radiation at room temperature. The specimens for TEM and HREM examinations were prepared by dispersing a powder in ethanol and collecting it onto holy carbon-coated grids. HREM examinations have been done only on the specimens before and after leaching at 30°C or 50°C for 0.5 hr. TEM and HREM investigations were carried out in a JEOL-2000 FX transmission electron microscope and a JEOL-2000 EX high resolution electron microscope respectively, both operating at 200 kV.

3. Results

As shown in Fig. 1a, in the X-ray diffraction spectrum of the rapidly solidified Raney Ni-Al starting alloy, the

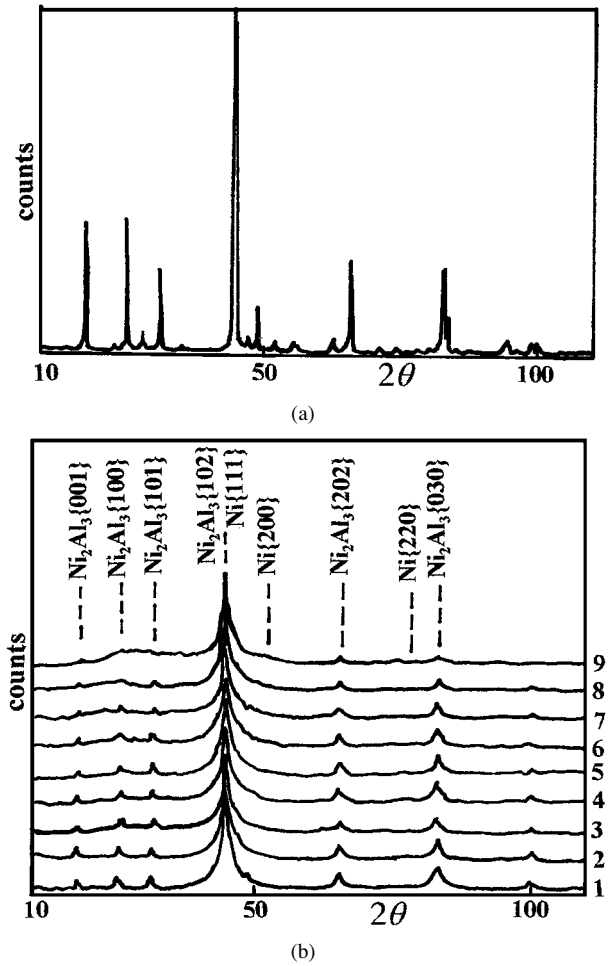

Figure 1 X-ray diffraction spectra (a) before leaching of the rapidly solidified Raney Ni-Al alloy; (b) after leaching for 1) 30 min. at 50°C; 2) 90 min. at 50°C; 3) 150 min. at 50°C; 4) 30 min. at 70°C; 5) 90 min. at 70°C; 6) 150 min. at 70°C; 7) 30 min. at 90°C; 8) 90 min. at 90° C; 9) 150 min. at 90°C.

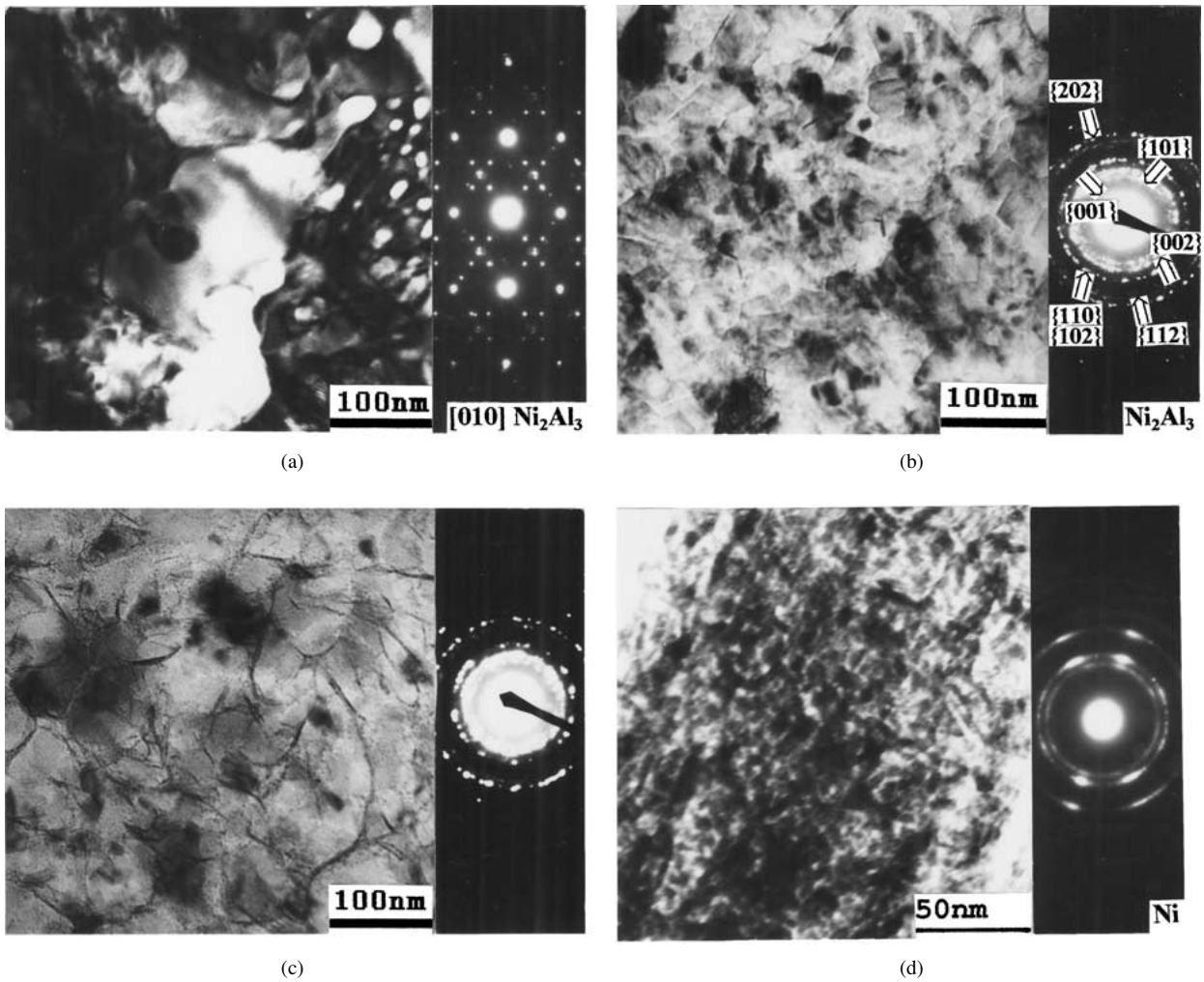

Figure 2 Electron micrographs and the corresponding diffraction patterns (a) before leaching and after leaching for (b) 150 min. at 50°C; (c) 150 min. at 70°C and (d) 150 min. at 90°C.

peaks with strong and medium intensities are those of Ni_2Al_3 reflections. The intensities of the peaks of $NiAl_3$ phase, which is another important source phase for Raney nickel catalyst, are very weak. Fig. 1b displays a comparison of the spectra after leaching under different conditions. It can be easily seen that the background grows up after leaching. With increasing leaching temperature, the intensity of Ni_2Al_3 phase decreases and diffused peaks of the product nickel emerge gradually. However even after 2.5 hours leaching at 90°C, the sharp peaks of Ni_2Al_3 are still faintly visible in the spectrum. The locations and the shapes of the Ni_2Al_3 peaks kept unchanged after leaching. The effect of a prolonging the leaching seems not as effective as increasing the temperature.

An electron micrograph and the corresponding diffraction pattern taken from the specimen before leaching are shown in Fig. 2a. It was from two Ni_2Al_3 domains oriented $\langle 0\,1\,0\rangle$ directions. In the alloy prepared by melt-spinning, Ni_2Al_3 grain size was not evenly distributed (0.2–0.01 μm), as could be seen in the figure. Frequently, a pattern of Ni_2Al_3 single grain or domains was obtained from one area and a ring pattern of polycrystalline Ni_2Al_3 from another area in a same specimen. Microstructural examination by TEM of the specimens after leaching under different conditions discovered that needle-form crystals were frequently observed, the length of which was longer at higher leaching temperature, as shown in Fig. 2b and c taken from the specimens after leaching for 2.5 hours at 50°C and 70°C. Leaching at 90°C leads to spheroidization of nickel grains generated, as can be seen in Fig. 2d, taken from the specimen leached at 90°C for 2.5 hours, the grain size of which was about 0.01 μm. Correspondingly, a texture-like polycrystalline nickel pattern appeared.

In order to clarify whether an intermediate phase, for instance, NiAl, Ni_3Al occurred during leaching, a series of selected area electron patterns with a common reciprocal direction were obtained at very beginning of leaching (30°C, 30 min). Two patterns and their indexing are shown in Fig. 3. The pattern in Fig. 3a is same as the one in Fig. 4c of Delannay's paper [8], which was indexed as one of $\langle 1\,1\,1\rangle$ axes of NiAl. If the pattern is indexed as one of Ni_2Al_3, its orientation should be one of $\langle 2\,4\,1\rangle = \langle 0\,2\,\bar{2}\,1\rangle$ axes, for instance [2 4 1]. The corresponding orientation of nickel crystal should be a high index $[\bar{7}\,0\,5]$ axis, and three families of {0 2 0} reflections of nickel in the pattern came from three different nickel crystallites in a texture structure. Rotating the specimen 35.5° around the reciprocal axis $(0\,2\,0)_{Ni} // (1\,0\,\bar{1}\,\bar{2})_{Ni_2Al_3}$, the pattern shown in

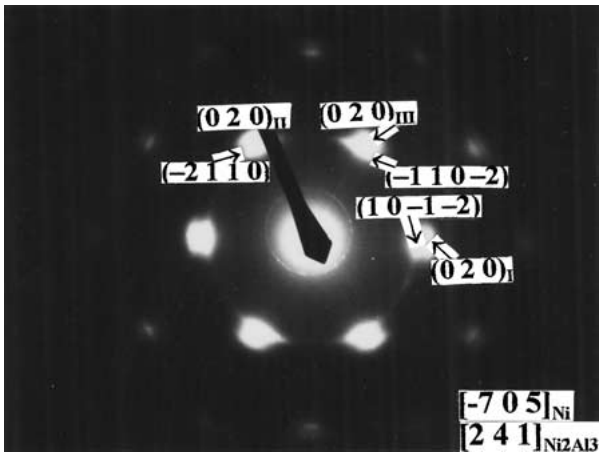

(a)

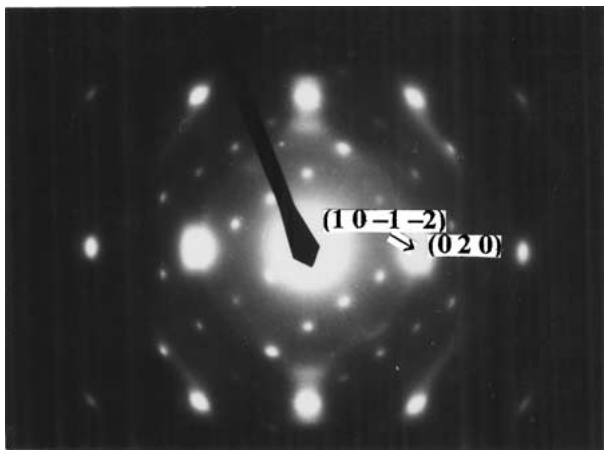

(b)

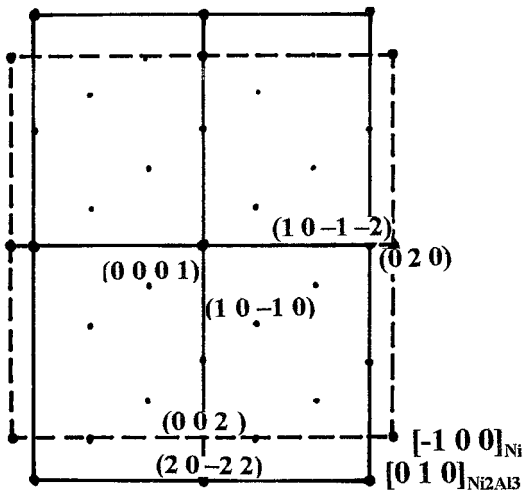

(c)

Figure 3 Composite electron diffraction patterns of Ni and Ni_2Al_3 with arced characteristics at very beginning of leaching (30°C, 30 min.) (a) the pattern in a textured structure, one of the solutions is $[2\,4\,1]_{Ni_2Al_3}$ // $[\bar{7}\,0\,5]_{Ni}$; and (b) the pattern obtained by rotating the specimen 35.5° around the reciprocal axis $(1\,0\,\bar{1}\,\bar{2})_{Ni_2Al_3}$ // $(0\,0\,2)_{Ni}$, (c) the schematic solutions of (b), the beam direction is $[0\,1\,0]_{Ni_2Al_3}$ // $[0\,\bar{1}\,0]_{Ni}$ // $[\bar{1}\,1\,0]_{NiAl}$.

Fig. 3b was obtained and indexed as shown in Fig. 3c. For Ni_2Al_3 structure [16], arranging in order of the intensities of reflections, there were {1 0 2}, {1 1 0}, {0 0 1}, {1 0 0}, {1 0 1}, {2 0 2}, {3 0 0}, {1 1 1}. Obviously, Fig. 3b should be a composite pattern of Ni_2Al_3 [0 1 0] and nickel $[\bar{1}\,0\,0]$ axis. Since the intensities of $(2\,0\,2)$, $(1\,0\,\bar{2})$ and (3 0 0) reflections of Ni_2Al_3 were too strong to be at right proportions, it seems that the

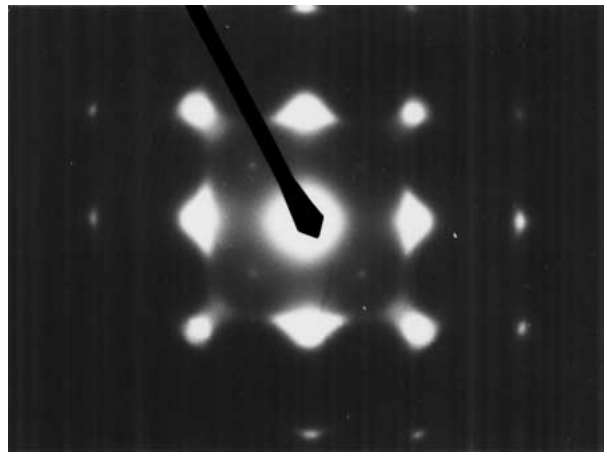

(a)

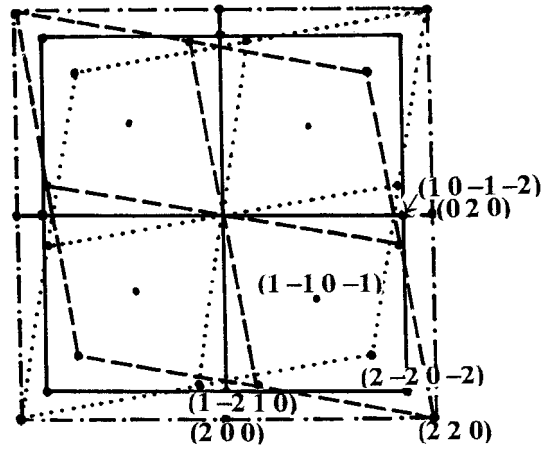

(b)

Figure 4 (a) A selected electron diffraction pattern and (b) schematic solution, the orientation of Ni_2Al_3 is $[2\,1\,1] = [1\,0\,\bar{1}\,1]$ and three sets of nickel domains coexisted, pattern is indexed as two sets of $\langle 0\,1\,1\rangle$ and one of $\langle 1\,0\,0\rangle$.

possibility of occurrence of the disordered cubic-NiAl structure could unlikely be ruled out. Assuming this is the case, its reflections would overlap $(2\,0\,2)$, $(1\,0\,\bar{2})$ and (3 0 0) of Ni_2Al_3. The corresponding zone axis of the disordered cubic-NiAl structure should be $[\bar{1}\,1\,0]$. The pattern in Fig. 3a is then possibly also a composite one with $[\bar{1}\,1\,1]$ axis of the NiAl phase. The angle calculated between $[\bar{1}\,1\,0]$ and $[\bar{1}\,1\,1]$ of the NiAl phase is 35.26°.

Another possible phase present could be Ni_3Al. However thorough examination of the diffraction patterns of specimens after leaching, none of Ni_3Al reflections were observed. Ni_3Al phase, which has a Cu_3Au-type ordered structure on the basis of FCC nickel lattice [16], and {100} reflections of Ni_3Al should be found at the midpoint of {200} reflection vectors of nickel phase. This could not be observed, e.g. in Fig. 3a and b. Thus, the formation of Ni_3Al during leaching could not be confirmed.

From one Ni_2Al_3 crystallite, nickel crystallites with different orientations would generate. These nickel crystallites obey an orientation relationship with Ni_2Al_3 source crystal as follows:

$$\langle 0\,0\,1\rangle_{Ni} \,//\, \langle 1\,0\,\bar{1}\,1\rangle, \langle 1\,\bar{2}\,1\,0\rangle, \langle 1\,0\,\bar{1}\,\bar{2}\rangle_{Ni_2Al_3}$$

$$\{0\,0\,1\}_{Ni} \,//\, \{1\,0\,\bar{1}\,1\}, \{1\,\bar{2}\,1\,0\}, \{1\,0\,\bar{1}\,\bar{2}\}_{Ni_2Al_3}$$

$$\text{with} \quad \{0\,\bar{7}\,5\}_{Ni} \,//\, \{0\,0\,0\,1\}_{Ni_2Al_3}$$

TABLE II The transformation matrices related Ni_2Al_3 with nickel, Ni_2Al_3 with NiAl and Ni_3Al_2 with nickel

	Transformation matrices(S)
Ni_2Al_3 with nickel	$\begin{pmatrix} 0.571 & 0.578 & 0.808 \\ -1.146 & -0.0033 & 0.0047 \\ 0.0034 & -1.132 & 0.803 \end{pmatrix}$
Ni_2Al_3 with NiAl	$\begin{pmatrix} 0.9878 & 0 & -0.9878 \\ -0.9878 & 0.9878 & 0 \\ 0.9792 & 0.9792 & 0.9792 \end{pmatrix}$
Ni_3Al_2 with nickel	$\begin{pmatrix} 1.071 & 0 & 0 \\ 0 & 1.071 & 0 \\ 0 & 0 & 0.921 \end{pmatrix}$

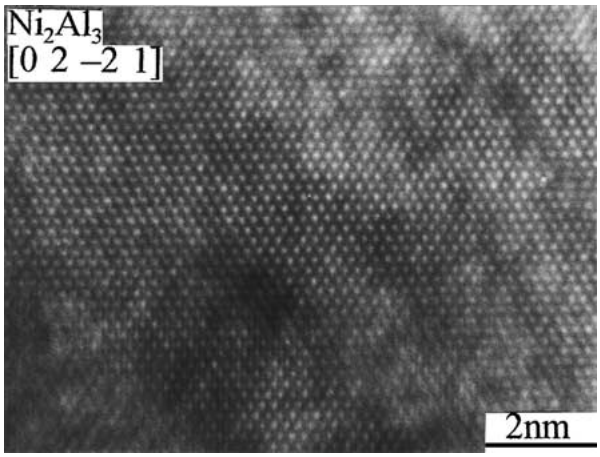

Figure 5 A HREM micrograph of Ni_2Al_3 in the Raney Ni-Al alloy.

These are consistent with the orientation relationships defined by Delannay [8] for nickel with NiAl and NiAl with the mother phase Ni_2Al_3. Table II presents their transformation matrices. Fig. 4 shows a case, where the orientation of Ni_2Al_3 is $[2\,1\,1] = [1\,0\,\bar{1}\,1]$ and three sets of nickel domains coexisted, patterns of which were indexed as two sets of $\langle 0\,1\,1\rangle$ and one of $\langle 0\,0\,1\rangle$.

As shown in Figs 3 and 4, arced reflection spots had been observed frequently on an electron diffraction pattern of the leached specimens. They have the following features:

(a) For all of the parallel reflections pairs of $\{2\,0\,0\}_{Ni} // \{1\,0\,-1\,2\}_{Ni_2Al_3}$ and $\{2\,0\,0\}_{Ni} // \{1\,1\,-2\,0\}_{Ni_2Al_3}$, the reflections of both the nickel and Ni_2Al_3 are arced (see Fig. 3a and b);

(b) In Fig. 3a, all of the spots identified as the reflections of Ni_2Al_3 are elongated along the direction perpendicular to $(1\,0\,-1\,-2)$ reciprocal vector,

(c) Increasing the leaching temperature, the arc characteristics of the reflections of nickel crystal appeared more clearly at first followed by texture-like patterns;

(d) Reflections of both nickel phase and Ni_2Al_3 on an electron diffraction pattern of the Raney nickel catalyst always manifest themselves as arcs, no streaks were observed in any case.

Fig. 5 shows a HREM micrograph of Ni_2Al_3 in the Raney Ni-Al alloy. The zone axis was $[2\,4\,1]$ of Ni_2Al_3 structure. Shown in Fig. 6 was a HREM micrograph of the specimen after leaching at 30°C for 0.5 hr, some crystalline clusters embedded in a Ni_2Al_3 crystallite. The corresponding electron diffraction pattern was the same as one shown in Fig. 4. The orientation of the Ni_2Al_3 crystallite was $[2\,1\,1] = [1\,0\,\bar{1}\,1]$. Careful measurement showed, that the areas marked A, B in the photograph were of $[1\,1\,0]$ of Ni_3Al_2 structure. An illustration of the area A and B and a lattice drawing of $[1\,1\,0]$ axis of nickel phase, for comparison, are shown in Fig. 6b and c respectively. The angle included between $(1\,\bar{1}\,1)$ and $(1\,\bar{1}\,\bar{1})$ for Ni_3Al_2 and nickel phase is 78.9° and 70.5° respectively. Ni_3Al_2 phase has a AuCu structure type [17] face-centered tetragonal arrangement, with lattice parameters 0.3773 and 0.3244 nm. Nickel atoms occupy 0,0,0 and 1/2,1/2,0 positions and 20% of the positions 1/2,0,1/2 and 0,1/2,1/2; the other 80% occupied by aluminum atoms. The present HREM investigation discovered that the face-centered tetragonal Ni_3Al_2 phase appeared at very beginning of leaching and coexisted with Ni_2Al_3 source phase.

Residual nano-scaled $NiAl_3$ crystallites were often observed to coexist with nickel nano-crystallites after leaching [15]. An interesting phenomenon was observed that leaching residue of $NiAl_3$ was hardly seen where nickel crystallites were twinned or multiple-twinned. It seems that in these cases the start alloy phase was Ni_2Al_3. Fig. 7 shows the multiple microtwins of nickel crystal marked with I, II and III, the size of which estimated to be about 1–5 nm. Take the thickness of the specimen as the length of the nickel grains (since moire fringes were not observed in the areas), the length of a nickel grain might be much larger than the size seen on the micrograph.

It can be seen clearly from Figs 6 and 7, that boundary region which has nearly the size of the nickel crystallites, 1–10 nm, with high intensity but low contrast existed and surrounded the nickel crystallites.

Intermediate phases of Ni_3Al and Ni_2Al were not observed in the specimens after leaching for 0.5 hr at 30°C or 50°C and did not present at the reaction front. The nickel crystallites produced in the leaching process seem to have crystallized perfectly and few crystal defects were found inside the nickel crystallites but the microtwin boundaries.

4. Discussions

The main start phase for leaching in the rapidly solidified Raney alloy was Ni_2Al_3 as verified by X-ray diffraction. The location and the sharp shape of the Ni_2Al_3 reflection peaks did not change after leaching. This suggests that the majority of grains of Ni_2Al_3 phase remained during leaching. The leaching process of Ni_2Al_3 phase was very different from that of $NiAl_3$ phase [15], in which grain fragmentation of mother phase to nano-scale grains would happen at the very beginning of leaching [18]. In contrast, the transformation of Ni_2Al_3 would be an advancing interface type during which the unchanged part of Ni_2Al_3 grains kept its original structure as verified by the X-ray and electron diffraction investigations. The leaching sequence of Ni_2Al_3 was likely a preferential dissolution followed by nickel reconstruction, as Bakker *et al.* [4] already suggested.

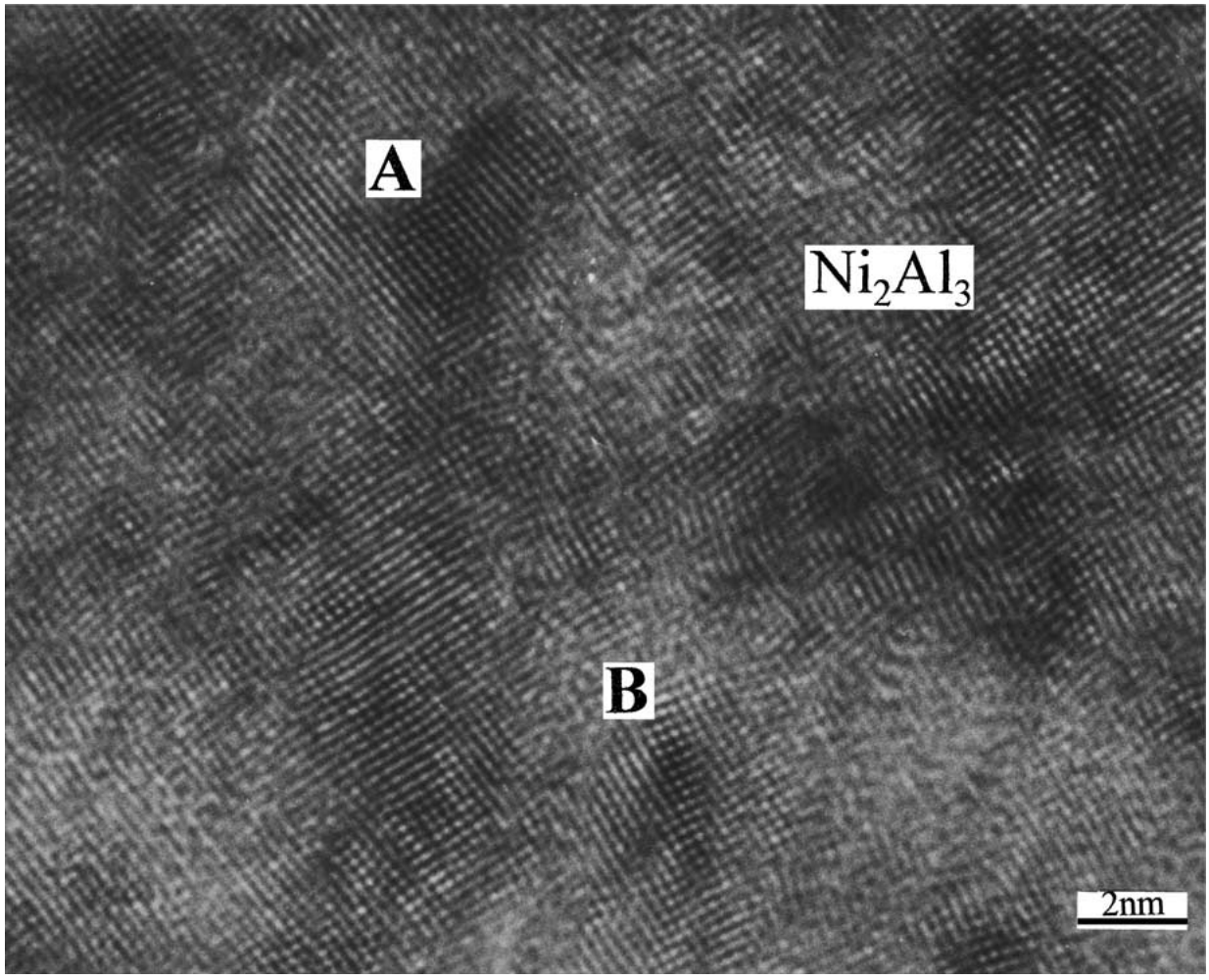

(a)

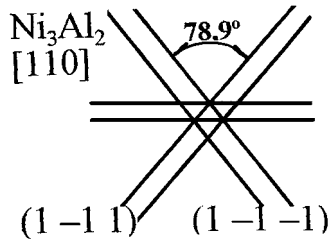

(b)

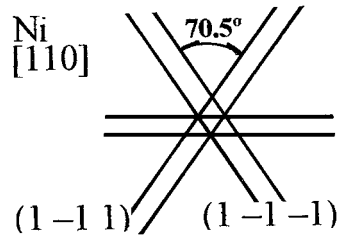

(c)

Figure 6 (a) A HREM micrograph of the specimen after leaching at 30°C for 30 min., the areas marked A and B were solved to be [1 1 0] axis of Ni_3Al_2. The orientation of the Ni_2Al_3 crystallite was $[2\,1\,1] = [1\,0\,\bar{1}\,1]$. The corresponding electron diffraction pattern was shown in Fig. 4; (b) An illustration of the areas A and B; (c) a lattice drawing of [1 1 0] axis of nickel phase. The angle included between $(1\,\bar{1}\,1)$ and $(1\,\bar{1}\,\bar{1})$ for Ni_3Al_2 and for nickel phase is 78.9° and 70.5° respectively.

A detailed analysis of a series of electron diffraction patterns revealed that the composite patterns obtained from the specimen after incomplete leaching can undoubtedly be indexed as those of Ni and Ni_2Al_3 in coexistence and there was no evidence of the presence of cubic NiAl and Ni_3Al phases. There remains the possibility of transitional presence of NiAl at the reaction front, more refined work is needed to obtain any possible evidence, if existed.

The present HREM investigation has shown that at very beginning of leaching, clusters of face-centered tetragonal Ni_3Al_2 appeared in the reaction front, embedded among Ni_2Al_3 crystallites. Ni_3Al_2 clusters might have existed, if any, in the transformation sequence as an transient product and soon transformed to nickel crystallites. Considering the crystal structures of these phases [16, 17], the transition mechanism could be easily understood. The structures of Ni_2Al_3 and NiAl differ by the existence of a vacancy layer on (0001) plane of Ni_2Al_3, which parallels to one of the planes {111} of NiAl. It should be noted that NiAl phase does not react with alkaline solution [1], thus aluminium leaching of Ni_2Al_3 can only happen to go through the vacancy layers from a surface edge towards the inner of a Ni_2Al_3 particle. Fig. 8a–c show respectively the atomic projection along $[1\,0\,\bar{1}\,1]$ direction and the atomic distributions on the planes $(1\,0\,\bar{1}\,\bar{2})$ and $(1\,\bar{2}\,1\,0)$ of Ni_2Al_3 structure. The dotted lines on the figures indicate a unit cell of nickel crystal, which obey the orientation relationship mentioned above between nickel and Ni_2Al_3 phases. It can be seen from the figures that a nucleus

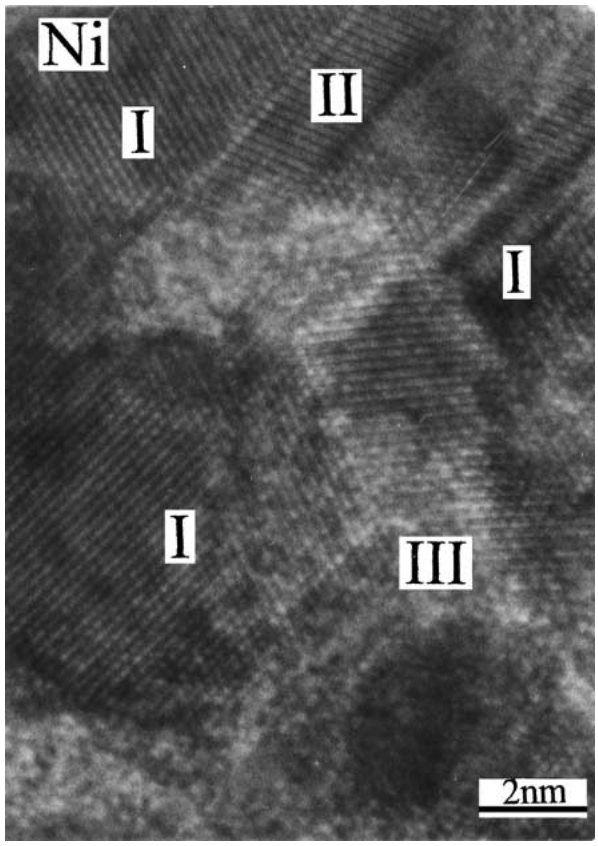

Figure 7 Microtwins of nickel crystal marked with I, II and III observed in the alloy after leaching at 50°C for 30 min.

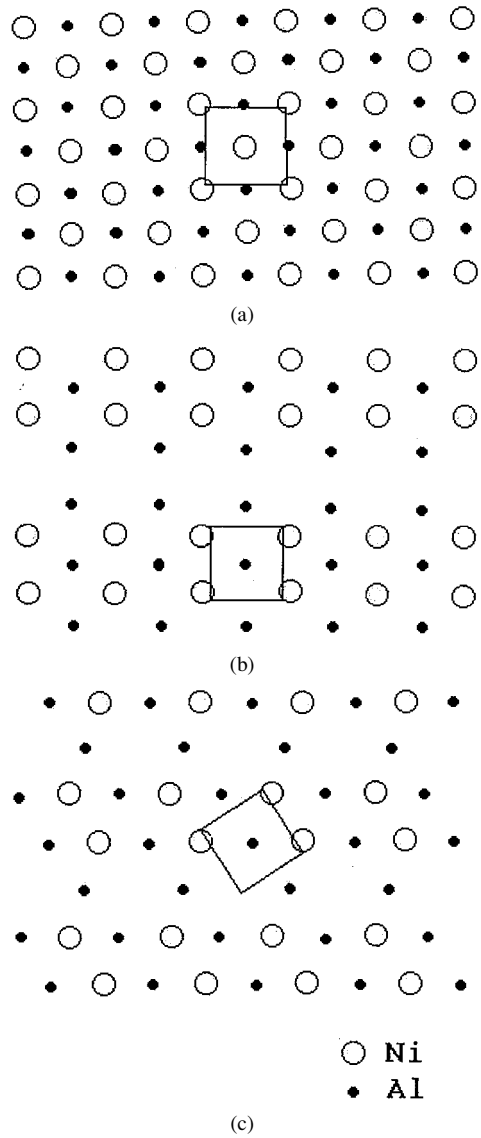

Figure 8 (a) the atomic projection along $[1\,0\,\bar{1}\,1]$ direction; the atomic distributions on (b) the plane $(1\,0\,\bar{1}\,\bar{2})$ and (c) the plane $(1\,\bar{2}\,1\,0)$ of Ni_2Al_3. The lines on the figures indicate a unit cell of nickel crystal, which follows the orientation relationship between nickel and Ni_2Al_3 phases.

with a centered square distribution on {1 0 0} plane of nickel crystal can easily be formed by compressing the plane distances $(1\,0\,\bar{1}\,\bar{2})$ and $(1\,\bar{2}\,1\,0)$ of Ni_2Al_3 phase 12.4% and 13.1% respectively. The atomic configurations on the planes $(1\,0\,\bar{1}\,\bar{2})$ and $(1\,\bar{2}\,1\,0)$ of Ni_2Al_3 phase are quite close to the one on {1 0 0} plane of nicel. Fig. 9a shows a subunit existing inside the Ni_2Al_3 structure, which has a face-centered tetragonal arrangement, the lengths of the unit sides are 0.402 and 0.2845 nm. Fig. 9b and c show respectively the unit cells of the Ni_3Al_2 phase and nickel. Obviously, the atomic configuration in the subunit is very similar to the one of the AuCu structure type Ni_3Al_2 [17]. Comparing the unit configurations and the parameters of Ni_3Al_2 (0.3773 and 0.3244 nm) with those of the subunit extracted from Ni_2Al_3 structure and nickel crystal (0.3254 nm), it can be seen that the structure of Ni_3Al_2 lies just in between. The orientation relationship between the Ni_3Al_2 and nickel crystal is given by $[1\,0\,0]_{Ni_3Al_2} // [1\,0\,0]_{Ni}$, $[0\,1\,0]_{Ni_3Al_2} // [0\,1\,0]_{Ni}$ and $[0\,0\,1]_{Ni_3Al_2} // [0\,0\,1]_{Ni}$. During the leaching process, what happened was that the aluminium diffused out and replaced by nickel, the diffusion of which was facilitated by the presence of vacancies formed in the leaching process.

Needle-form morphology was frequently observed in a specimen after leaching at 50° and 70°C. The length of the needles increased with increasing leaching temperature. It was discovered experimentally that diffraction spots of nickel phase generated always manifested themselves in arcs, not streaks. It is known [19] that precipitates of nano-scale size oriented in a limited ways contribute to a 'single crystal' pattern. The orientation relaxing with the size effect made the angle of a diffraction beam spread. The arced intensity distribution of reflections of the nano-scale nickel crystallites occurred could be interpreted in a similar mechanism The leaching product with a needle morphology and each reciprocal lattice spot became a thin sheet perpendicular to the needles. Supposing the needles parallel to $[0\,1\,0]$ or $[1\,0\,\bar{2}]$ directions of Ni_2Al_3, all of the reciprocal sheets should be perpendicular to the corresponding direction. Intersection of the reciprocal sheets with the reflection sphere results in the arc characteristics of intensity distribution as shown in Figs 3 and 4. The reflection spots for all of the parallel reflections pairs of $\{2\,0\,0\}_{Ni} // \{1, 0\,\bar{1}\,\bar{2}\}_{Ni_3Al_2}$ and $\{2\,0\,0\}_{Ni} // \{1\,\bar{2}\,1\,0\}_{Ni_3Al_2}$ elongated perpendicularly to the corresponding reciprocal vectors. And the diffraction spots, which appeared on the pattern shown in Fig. 3a, elongated perpendicularly to $\{1\,0\,\bar{1}\,2\}$ reciprocal vector. It can be drawn from the atomic configurations in Fig. 8a–c, that nickel crystallites generate preferentially along $[0\,1\,0]$ or $[1\,0\,\bar{2}]$ directions of Ni_2Al_3

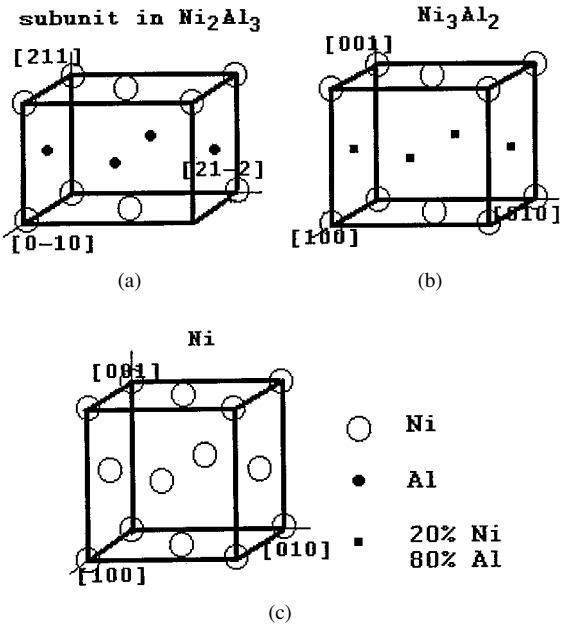

Figure 9 The atomic configuration in (a) a subunit existing inside the Ni_2Al_3 structure, the lengths of the unit sides are 0.405, 0.402 and 0.2845 nm; (b) an unit of the AuCu structure type-Ni_3Al_2 $a = 0.3773$, $c = 0.3244$ nm and (c) an unit cell of nickel crystal, $a = 0.3523$ nm.

and the needles of nickel generated parallel to either of the directions.

At higher temperature (90°C) the nickel grains generated spheroidized and a textured nickel polycrystalline pattern was easily obtained everywhere. The texture feature of polycrystalline patterns of nickel generated during aluminium leaching of Raney alloys have been reported previously [7] and it seemed that 90°C was high enough for nickel to recrystallize in the special chemical environment.

A large number of nickel nuclei were situated at the reaction front during leaching and grew up to nano-scale nickel crystallites. Therefore, the transformation, agrees with Bakker *et al*. [5], that it proceeds by preferential dissolution of Ni_2Al_3 at the reaction front followed by generation of nickel crystallites. The microtwins observed in a HREM examination of specimens prepared by aluminum leaching of the rapidly solidified Raney alloy are formed by growth twinning, a phenomenon observed in aluminium during freezing from melt and more often in many minerals, the phenomenon known as polysynthetic twinning, and now observed in nickel recrystallization by the removal of other component or components in a nickel alloy.

Another distinguishing feature of the catalyst structure discovered in the present study is that a poorly crystallized boundary region surrounds the nano-scale nickel crystallites. Intensity of these boundary regions in a HREM image was always higher than the crystallites regions. The imaging contrast of these boundary regions in the HREM technique consists of the phase and the density-thickness contrasts. The idea that the boundary regions had a low atomic density could be easily accepted. The perfection of the nickel crystallites that was observed in a HREM image demonstrates that excessive aluminium in the nickel alloy and a large number of vacancies should have aggregated into the boundary regions. As a result, the boundary regions have a structure being rich in pores. Hamar-Thibault *et al*. [7] observed crystallites of the oxide or hydroxide of aluminium which was situated in a particular area of the catalyst surface. The porous structure at the boundary regions provides passages for the reactants and increases the active surface area, thus causing a high hydrogenation catalytic activity.

5. Conclusions

1. Ni_2Al_3 is the main phase in a rapidly solidified Raney NiAl alloy;

2. The structural change during leaching of Ni_2Al_3 phase is an advancing interface type process. Clusters of AuCu- structured face-centered tetragonal Ni_3Al_2 are possibly the only intermediate phase. An explanation based on an analysis of atomic configurations of phases Ni_2Al_3, Ni_3Al_2 and Ni, for the reaction during leaching and the arc morphology of diffraction spots is proposed;

3. Microstructure of the Raney nickel catalyst consists of nanoscale twinned nickel crystallites, residue of source phases, surrounded by nanoscale boundary areas;

4. The nickel crystallites generated during leaching obey the following orientation relationship with the source Ni_2Al_3 phase:

$$\langle 0\,0\,1\rangle_{Ni} // \langle 1\,0\,\bar{1}\,1\rangle, \langle 1\,\bar{2}\,1\,0\rangle, \langle 1\,0\,\bar{1}\,\bar{2}\rangle_{Ni_2Al_3}$$

$$\{0\,0\,1\}_{Ni} // \{1\,0\,\bar{1}\,1\}, \{1\,\bar{2}\,1\,0\}, \{1\,0\,\bar{1}\,\bar{2}\}_{Ni_2Al_3}$$

$$\text{with} \quad \{0\,\bar{7}\,5\}_{Ni} // \{0\,0\,0\,1\}_{Ni_2Al_3}$$

5. The nano-scale structure of the Raney nickel catalyst provides an excellent hydrogenation catalytic activity and selectivity of the catalyst.

Acknowledgements

Partially financial support from the Chinese Institute of Petroleum Processing Research is gratefully acknowledged. The experimental materials were supplied by Dr. Baoning Zong and discussions with Professors Enze Min, Wanzhen Lu, Drs. Baoning Zong and Xuhong Mu are deeply appreciated.

References

1. FRASER, *Trans. Electrochem. Soc.* **71** (1937) 425.
2. G. D. ULIANOVA, Dissertation, in Russian, Kiev University (1972).
3. S. D. ROBERTSON, J. FREEL and R. B. ANDERSON, *J. Catal.* **24** (1972) 130; S. D. ROBERTSON and R. B. ANDERSON, *ibid.* **23** (1971) 286.
4. J. FREEL, W. J. M. PIETERS and R. B. ANDERSON, *ibid.* **16** (1970) 281.
5. M. L. BAKKER, D. J. YOUNG and M. S. WAINWRIGHT, *J. Mater. Sci.* **23** (1988) 3921.
6. R. SALLOULAS and V. TRAMBOUSE, *Bull. Soc. Chim. Fr.* **5** (1964) 985.
7. S. HAMAR-THIBAULT, J. THIBAULT and J. C. JOUD, *Z. Metallkd.* **83** (1992) 258.
8. F. DELANNAY, *Reactivity of Solids* **2** (1986) 235.

9. J. GROS, S. HAMAR-THIBAULT and J. C. JOUD, *Surface and Interface Analysis* **11** (1988) 611.
10. *Idem., J. Mater. Sci.* **24** (1989) 2987.
11. L. N. GUSEVA and E. S. MAKAROV, *Dokl. Akad. Nauk SSSR* **77** (1951) 615.
12. F. REYNAUD, *J. Appl. Cryst.* **9** (1976) 263.
13. E. IVANOV, G. V. GOLUBKOVA and T. F. GRIGORIEVA, *Reactivity of Solids* **8** (1990) 73.
14. E. IVANOV, S. A. MAKHLOUF, K. SUMIYAMA, H. YAMAUCHI, K. SUZUKI and G. GOLUBKOVA, *J. Alloys and Compounds* **185** (1992) 25.
15. R. WANG, Z. L. LU and T. KO, to be published.
16. A. J. BRADLEY and A. TAYLOR, *Phil. Mag.* **23** (1937) 1049.
17. TAYLOR, *J. Appl. Phys.* **5** (1972) 201.
18. Z. L. LU, R. WANG, T. KO, H. CHEN, X. H. MU and B.N. ZONG, *Chinese J. Catal.* **18** (1997) 110.
19. P. B. HIRSCH, A. HOWIE, R. B. NICHOLSON, D. W. PASHLEY and M. J. WHELAN, "Electron Micrscopy of Thin Crystals" (The Butterworth Co., London, 1965) p. 129.

Received 11 August 2000
and accepted 8 August 2001